

RESEARCH ARTICLE

Regulation of Host Regulatory T Cell Differentiation by emu-let-7-5p in *Echinococcus multilocularis* Infection Through Targeting NF κ B2

Liqun Wang¹  | Keke Wu¹  | Li Li¹  | Tharheer Oluwashola Amuda¹  | Yixuan Wu¹  |
 Guiting Pu¹  | TingLi Liu¹  | Shanling Cao¹  | Hong Yin^{1,2}  | Baoquan Fu^{1,2}  | Hongbin Yan^{1,3}  |
 Xuenong Luo^{1,2} 

¹State Key Laboratory for Animal Disease Control and Prevention, National Para-Reference Laboratory for Animal Echinococcosis, Key Laboratory of Animal Parasitology of Gansu Province, Lanzhou Veterinary Research Institute, Chinese Academy of Agricultural Sciences (CAAS), Lanzhou, China | ²Jiangsu Co-Innovation Center for the Prevention and Control of Important Animal Infectious Disease and Zoonoses, Yangzhou University, Yangzhou, China | ³College of Veterinary Medicine, Lanzhou University, Lanzhou, China

Correspondence: Baoquan Fu (fubaoquan@caas.cn) | Hongbin Yan (yanhongbin@caas.cn) | Xuenong Luo (luoxuenong@caas.cn)

Received: 1 January 2025 | **Revised:** 23 March 2025 | **Accepted:** 24 April 2025

Funding: This study was financially supported by the Gansu Provincial Youth Science and Technology Fund Program (25JRRA443), the National Key Research and Development Program of China (2023YFD1802401), the National Natural Science Foundation of China (32072889), the Agricultural Science and Technology Innovation Program (ASTIP) of CAAS (CAAS-ASTIP-2021-LVRI), and the Major Science and Technology Project of Gansu Province (22ZD6NA001 and 23ZDNA007).

Keywords: *E. multilocularis* | emu-let-7-5p | NF κ B2 | Treg cell differentiation

ABSTRACT

Regulatory T cells (Treg) play a crucial role in creating an immunosuppressive microenvironment surrounding the metacestode during chronic alveolar echinococcosis (AE). However, the mechanisms by which *E. multilocularis* induces Treg differentiation, particularly the role of parasite-derived microRNAs (miRNAs), remain largely unexplored. Here, we demonstrate that *E. multilocularis* can significantly induce the differentiation of Treg in mice. Emu-let-7-5p is upregulated in peripheral blood lymphocyte cells (PBLC) and splenic lymphocytes of *E. multilocularis*-infected mice. Exosomes enriched with emu-let-7-5p were found to upregulate the expressions of Treg markers. Conversely, exosomes collected following the knockdown of worm-derived emu-let-7-5p via RNA interference resulted in a reversal of Treg marker expression in PBLC. Mechanistically, emu-let-7-5p regulates Treg differentiation by targeting NF κ B2. Knockdown of emu-let-7-5p in *E. multilocularis*-infected mice resulted in diminished Treg differentiation, leading to a significant reduction in worm load. These findings reveal that emu-let-7-5p drives Treg differentiation by suppressing NF κ B2, representing a novel immune evasion strategy of *E. multilocularis*. Sustained inhibition of parasite-derived emu-let-7-5p may provide a therapeutic avenue for controlling AE progression.

1 | Introduction

Alveolar echinococcosis (AE) is a severe and potentially lethal zoonotic parasitic disease caused by the metacestode of *E. multilocularis*. This disease is primarily found in the northern hemisphere, particularly in regions such as northern and central Europe, North America, and Western China [1, 2]. The life cycle of *E.*

multilocularis involves canids as definitive hosts and small rodents as intermediate hosts. Humans are aberrant intermediate hosts infected through oral ingestion of infectious eggs shed in the feces of definitive hosts. AE manifests as infiltrative hepatic lesions with malignant tumor-like progression. In advanced stages, AE affects the whole liver and metastasizes to other organs via the bloodstream and lymphatic system [3], leading to portal hypertension,

pulmonary echinococcosis, cerebral echinococcosis, and even death [4, 5]. The global burden of AE is estimated at 18 235 cases annually, leading to a staggering loss of 666 434 disability-adjusted life years (DALYs) [6]. Notably, China accounts for 91% of global AE cases and 95% of associated DALYs [7]. This highlights the significant threat that AE poses to both human and animal health. Current treatment strategies primarily involve surgical excision, complemented by the administration of benzimidazoles both before and after surgery [8]. Despite these interventions, the prognosis for AE patients remains poor, with limited success in achieving favorable long-term outcomes [9]. Therefore, there is an urgent need for the development of new and more effective treatment options for AE.

Through host–parasite coevolution, *E. multilocularis* has evolved sophisticated strategies to modulate host anti-infective immunity, thereby ensuring its long-term survival in the challenging environment of the host. Increasing evidence suggests that the differentiation and expansion of Treg represent a significant route through which *E. multilocularis* regulates the host immune response [10–12]. Treg play a crucial role in maintaining immune homeostasis and protecting the host from a potentially pathogenic immune response [13].

Previous studies have indicated that the population of CD4⁺CD25⁺ Treg is upregulated in cases of human chronic AE [14, 15], which is thought to correlate with a reduction in immune responses to specific antigens and/or the suppression of proinflammatory cytokine production, particularly through the secretion of high levels of anti-inflammatory cytokines such as interleukin (IL)-10 and transforming growth factor-beta (TGF- β) [16]. Murine infection models recapitulate this Treg expansion in splenic/peritoneal compartments [17, 18], further implicating Treg induction as a key immune evasion mechanism.

Recent findings have revealed that the *E. multilocularis* activin A homolog (EmACT), a component of the excretory/secretory product (ESP) from *E. multilocularis*, promotes the expansion of Foxp3⁺ Treg and enhances the production of the immunosuppressive IL-10 by host CD4⁺ T cells [11]. These results underscore the ability of *E. multilocularis* to induce T cells to differentiate into Treg, highlighting its intricate strategies for immune evasion.

Exosomes are nanosized membrane vesicles secreted by various cell types, containing a diverse array of biomolecules, including mRNAs, miRNA, proteins, and DNA fragments. They play a crucial role in numerous biological processes, such as cell–cell signaling and the transfer of molecules between cells [19]. An increasing body of research indicates that parasitic exosomes can deliver their contents into host cells, which parasites may exploit to modulate the host immune response for their survival [20].

MicroRNAs (miRNAs) are small, endogenous non-coding RNA molecules that significantly influence cellular differentiation, proliferation, pathogenesis, and disease susceptibility [21]. For instance, miR-155 promotes Treg differentiation by targeting suppressor of cytokine signaling 1 (SOCS1) [22, 23]. In vitro studies indicate that inhibiting miR-155 expression can lead to increased SOCS1 levels and enhanced immune function in induced Treg (iTreg) [22]. Similarly, miR-146a regulates Treg differentiation by inhibiting signal transducer and activator of

transcription 1 (STAT1). A reduction in miR-146a levels can impair Treg differentiation, mitigate immune rejection, and promote the survival of transplanted donor hearts [24]. Moreover, the miR-15/16 cluster restricts Treg differentiation by targeting interferon regulatory factor 4 (IRF4). The loss of these miRNAs in Treg has been associated with diminished immune responses during neuroinflammation and in response to both infectious and non-infectious challenges [25]. These findings collectively suggest that miRNAs play a pivotal role in the regulation of Treg differentiation.

Among evolutionarily conserved miRNA families, the let-7 family plays a pivotal role in shaping Treg biology through direct targeting of key transcription factors and signaling nodes, including c-Myc, Lin28, and Foxp3 [26, 27]. This conserved miRNA family also coordinates immune homeostasis by precise modulation of TGF- β /NF- κ B signaling cascades as well as regulates the Th17/Treg balance through targeting STAT3 and IL-6R [28, 29]. Intriguingly, *E. multilocularis* let-7 (emu-let-7-5p), a homolog of the let-7 family, exhibits striking abundance in both *E. multilocularis* and its exosomes [30, 31]. However, the specific role of emu-let-7-5p in modulating Treg cell differentiation by *E. multilocularis* remains largely unexplored. The objective of this study was to elucidate the mechanism by which emu-let-7-5p, derived from exosomes of *E. multilocularis*, regulates the differentiation of host Treg. Our findings demonstrate that emu-let-7-5p from the exosomes of *E. multilocularis* promotes the differentiation of host Treg cells and enhances the production of immunosuppressive cytokines, specifically IL-10 and TGF- β , through the targeting of NF κ B2. This consequently results in the restriction of worm growth. The results of this study provide insight into the mechanisms underlying parasite–host interactions, highlighting how *E. multilocularis* may evade host immune attacks.

2 | Materials and Methods

2.1 | Reagents, Cells, and Parasites

The NF κ B2 siRNA, scrambled siRNA, emu-let-7-5p mimics, and mimics nc were purchased from Sangon Biotech (Shanghai, China). The fluorescently labeled small interfering RNAs (siRNAs) specifically targeting emu-let-7-5p and a scramble control sequence were designed and synthesized by Sangon Biotech (Shanghai, China). TGF- β was purchased from BioLegend and used at a final concentration of 5 ng/mL. IL-2 was purchased from Peprotech and used at a final concentration of 20 ng/mL. HEK293T cells were obtained from National Collection of Authenticated Cell Cultures (Shanghai, China). Cells were authenticated by STR profiling. *E. multilocularis* protoscolices utilized in the present study were sourced from Mongolian gerbils infected with AE, following the methodology outlined by Wang et al. [32].

2.2 | Animals and Ethics Statement

Female BALB/c mice (6–8 weeks old) were purchased from the Laboratory Animal Center of Lanzhou Veterinary Research Institute. The mice were housed in specific-pathogen-free (SPF)

facilities, where they were maintained under controlled conditions, including a temperature of $22^{\circ}\text{C} \pm 2^{\circ}\text{C}$ and humidity levels appropriate for their care. A 12-h (h) light/dark cycle was implemented, and the animals had unlimited access to a standard diet and fresh water.

The animal study followed the guidelines outlined by the Good Animal Practice of Animal Ethics Procedures and Guidelines of the People's Republic of China. Approval for the protocol was obtained from the Animal Ethics Committee of Lanzhou Veterinary Research Institute, Chinese Academy of Agricultural Sciences (Permit No. LVRIAEC2023-018).

2.3 | rAAV8 Design and Production

A sponge sequence, a DNA fragment containing four complementary sequences (5'-AGACATTCGAGTTCTACCTCA-3') against emu-let-7-5p connected by a linker (5'-GGGTCCC-3'), was designed, synthesized, and cloned into the AAV8-CMV-GFP-mirRNA plasmid to construct a recombinant vector, pAAV8-si-emu-let-7-5p. The empty AAV8-CMV-GFP-mirRNA plasmid was used as a control, namely pAAV8-si-control. After verification by sequencing, the recombinant plasmids were introduced into HEK293T cells, and the efficiency of the sponge sequence interfering with emu-let-7-5p was assessed by reverse transcription-quantitative polymerase chain reaction (RT-qPCR). The two plasmids were then packaged into the recombinant adeno-associated virus serotype 8 (rAAV8), named rAAV8-si-emu-let-7-5p and rAAV8-si-control, to facilitate their delivery into the liver of mice for the study of the effects of emu-let-7-5p on Treg differentiation during *E. multilocularis* infection. Plasmid construction, rAAV8 packaging, and rAAV8 titer determination were conducted by Vigene Biosciences (Shandong, China).

2.4 | Animal Infection

A total of 96 female mice were randomly assigned to two groups: the infection group ($n=48$) and the control group ($n=48$). Mice in the infection group received an intraperitoneal injection of 1 000 protoscolices, while those in the control group were administered an equivalent volume of phosphate-buffered saline (PBS). At 30, 60, 90, and 180 days post-infection (dpi), 12 mice from each group were euthanized, the blood samples from four mice were pooled, and peripheral blood lymphocyte cells (PBLC) were isolated using the Mouse Peripheral Lymphocyte Separation Kit (TBD Sciences, Tianjing, China). Spleen cells from both control and *E. multilocularis*-infected mice were isolated by grinding the spleens in 5 mL of PBS. The cells were then washed twice and resuspended in PBS for flow cytometry.

To inhibit emu-let-7-5p in vivo, a total of 33 mice were randomly divided into three groups ($n=11$ per group): the PBS group, the rAAV8-si-control group, and the rAAV8-si-emu-let-7-5p group. Each mouse received 200 μL of PBS or 2×10^{11} viral genomes (vg) of rAAV8-si-control or rAAV8-si-emu-let-7-5p in 200 μL of PBS, respectively. At 15 dpi, one mouse from each group was randomly selected for evaluation of GFP expression in liver

tissue. The remaining mice were then intraperitoneally inoculated with 1 000 protoscolices per mouse. At 90 dpi, all mice were humanely euthanized, and tissue samples were collected for subsequent analysis.

2.5 | *E. multilocularis* Exosomes Isolation

Exosomes derived from *E. multilocularis* protoscolices were prepared following established protocols [33]. Briefly, protoscolices were cultured in RPMI-1640 medium supplemented with 1% penicillin-streptomycin (Hyclone, USA) and 10% exosome-depleted fetal bovine serum (FBS, VivaCell, Germany) for 24 h at 37°C in a 5% CO_2 atmosphere. After incubation, the culture supernatant was collected and subjected to centrifugation at 300g for 10 min (min) and followed by centrifugation at 2 000g for 30 min to eliminate cellular debris and protoscolices. The supernatant was then further centrifuged at 10 000g for 1 h, and finally, a last centrifugation was performed at 110 000g for 2 h to isolate exosomes. The resulting pellet (exosomes) was resuspended in 100 μL of PBS, and the protein concentration of the exosomes was quantified using the Pierce BCA Protein Assay Kit (Thermo Fisher Scientific, USA). Meanwhile, the endotoxin level in the exosome preparation was assessed using the Toxinsensor Chromogenic LAL Endotoxin Assay Kit (GenScript, China).

2.6 | Transmission Electron Microscopy (TEM)

The morphology of *E. multilocularis* exosomes was analyzed using transmission electron microscopy (TEM, Hitachi, Japan). In short, 10 μL of exosomes were fixed onto formvar/carbon-coated nickel grids (Agar Scientific Ltd., United Kingdom) and then stained with 3% glutaraldehyde (Solarbio, Beijing, China) for 10 s at room temperature. Imaging was conducted using a Hitachi transmission electron microscope operating at 80 kV.

2.7 | Nanoparticle Tracking Analysis (NTA)

The size distribution of *E. multilocularis* exosomes was measured using the nanoparticle tracking analysis (NTA). Briefly, 1 μL of exosomes was diluted in 1 mL of PBS and loaded into the ZETASIZER NANOS (NTA, Malvern, United Kingdom). The exosome particles were tracked and sized based on Brownian motion and the diffusion coefficient. The diameter size and particle concentration of exosomes were analyzed using the ZetaView 8.02.28 software.

2.8 | Exosomes Uptake

Exosomes uptake of PBLC and splenic lymphocytes was analyzed by DiD staining assay using the kit according to the manufacturer's instructions. Briefly, 10 μL exosomes were mixed with 1 μL of DiD fluorescent dye (Abcam, United Kingdom) and incubated for 20 min at 37°C in the dark. Then, the DiD-labeled exosomes were incubated with cells for 6 h, and the cellular location of the exosomes was observed by a fluorescence microscope (TCS SP8, Leica, Germany). 4',6-Diamidino-2-phenylindol

(DAPI) was used to stain the nuclei of the PBLC and splenic lymphocytes.

2.9 | Delivery of RNAi Molecules Into *E. multilocularis* Protoscolices

The fluorescently labeled siRNA sequences are as follows: emu-let-7-5p siRNA, 5'-FAM-AGACAUUCGAAACACUACC UCA-3'; scrambled siRNA, 5'-FAM-AGACCUCAUGCUGCA UCGCUCA-3'. The RNA interference (RNAi) was conducted following the protocols established by Mizukami et al. [34] and Liu et al. [35] with minor modifications. In brief, 2 000 protoscolices were incubated in solutions containing either emu-let-7-5p siRNA (5 μ M) or scrambled control siRNA (5 μ M), both dissolved in RPMI-1640 medium supplemented with 1% penicillin–streptomycin (Hyclone, USA) and 10% exosome-depleted FBS (VivaCell, Germany). Additionally, a control was incubated with RPMI-1640 and the above supplements. After 2 h of incubation at 37°C and with 5% CO₂, protoscolices were washed three times with PBS and then resuspended in 200 μ L of electroporation buffer (Bio-Rad, USA) containing a concentration of 5 μ M siRNA. Electroporation was performed at 200 V and 1 000 μ F for 20 ms using an exponential decay pulse in a 4 mm electroporation cuvette (Bio-Rad, USA). Following electroporation, the samples were incubated at 37°C for 1 h. Subsequently, 1 mL of FBS-free RPMI-1640 medium was added to each cuvette, and the contents were transferred to 24-well plates, and the uptake efficiency of siRNA by the protoscolices was visualized using a fluorescence microscope (Zeiss, Germany). Additionally, the culture supernatants were collected at 24, 48, and 72 h post electroporation for exosome isolation. The protoscolices from each group were collected at 24 h post electroporation.

2.10 | Total RNA Extraction and RT-qPCR

Total RNA was extracted using the TRIzol Reagent (Thermo Fisher Scientific, USA) following the manufacturer's protocols, and RT-qPCR was conducted as described by Wang et al. [32] The relative expression levels of genes were determined using the 2^{- $\Delta\Delta$ Ct} method. All primers used in this study are listed in Table S1.

2.11 | Western Blotting

Total protein was extracted from cells and exosomes using RIPA lysis buffer (Thermo Fisher Scientific, USA), and the protein concentration was quantified using the BCA protein assay kit (Vazyme, China). A total of 30 μ g of protein was separated by 12% SDS-PAGE and subsequently transferred onto PVDF membranes. Following a blocking step with 5% non-fat milk, the membranes were incubated overnight at 4°C with primary antibodies: anti- β -actin (1: 5 000, Abcam, United Kingdom), anti-NF κ B2 (1: 1 000, Santa Cruz, USA), and anti-14-3-3 (1:1 000) antibodies. Afterward, the membranes were treated with the HRP-conjugated secondary antibodies, specifically goat anti-mouse IgG-HRP (1: 4 000, Biodragon, China) and goat anti-rabbit IgG-HRP (1: 4 000, Biodragon,

China) antibodies for 50 min. The protein bands were visualized using an Electrochemical Luminescence (ECL) Kit (Beyotime, China). Finally, the intensities of the blots were analyzed using ImageJ software.

2.12 | Enzyme-Linked Immunosorbent Assay (ELISA)

Blood samples collected from both the control and experimental groups were centrifuged at 3 000 rpm for 10 min. The sera were then separated and stored at –80°C until further analysis. The concentrations of IL-10, TGF- β , and Foxp3 in the serum samples were detected using ELISA Kits (RayBiotech, USA), following the manufacturer's protocols. Each assay was conducted in triplicate to ensure the accuracy and reliability of the results.

2.13 | Cell Transfection

1 \times 10⁶ PBLC were seeded into each well of the 6-well plates. After overnight incubation with 5% CO₂ at 37°C, NF κ B2 siRNA (si-NF κ B2), emu-let-7-5p mimics, NF κ B2 overexpression plasmid (pEGFP-N1-NF κ B2), and negative control were transfected into PBLC using Lipofectamine 3000 transfection reagent (Thermo Fisher Scientific, USA). The final concentration of pEGFP-N1-NF κ B2 was 2 000 ng/mL, and all treatment concentrations of NF κ B2 siRNA, scramble siRNA, emu-let-7-5p mimics, and mimics nc were 50 nM. The sequences of siRNA and scramble siRNA are listed in Table S2. After 24 h of transfection, the cells were harvested for further assays.

2.14 | Identification of emu-let-7-5p Targets

To systematically identify high-confidence targets of emu-let-7-5p, we integrated three complementary miRNA prediction algorithms: miRanda (version August 2010; <http://www.microrna.org/>), TargetScan (version 7.2; <http://www.targetscan.org/>), and PicTar (vertebrate algorithm; <http://pictar.mdc-berlin.de/>) [36]. Stringent parameters were applied to minimize false positives: miRanda was executed with a binding energy threshold of ≤ -18 kcal/mol and a sequence alignment score cutoff of ≥ 150 , prioritizing thermodynamically stable miRNA-mRNA interactions. TargetScan predicted focused on conserved 8-mer and 7-mer seed matches, requiring a context++ score ≤ -0.4 to ensure functional relevance. PicTar predictions demanded strict phylogenetic conservation across ≥ 3 vertebrate species and a score threshold of ≥ 7.0 , emphasizing evolutionarily conserved binding sites. Targets predicted by all three algorithms were classified as high-confidence candidates.

2.15 | Dual Luciferase Reporter Assay

The wild-type NF κ B2 coding sequence (CDS), referred to as CDS-WT, and the mutant NF κ B2 CDS referred to as CDS-MUT, along with the wild-type NF κ B2 CDS-3' untranslated region (UTR), designated as CDS-3'UTR-WT, and mutant

NF κ B2 CDS-3'UTR, designated as CDS-3'UTR-MUT, were cloned into the dual-luciferase reporter vector pmirGLO (Sangon Biotech, China). Each recombinant plasmid was then co-transfected with either emu-let-7-5p mimics or mimics nc into HEK293T cells using Lipofectamine 3000 Transfection Reagent (Thermo Fisher Scientific, USA). After 24 h of transfection, the activity levels of renilla and firefly luciferase were measured using the Promega Glomax 96 (Promega Corporation, Wisconsin, USA).

2.16 | Cell Preparation and Flow Cytometry

Enrichment of CD4⁺CD25⁺ regulatory T cells from mouse splenocytes was conducted using the MojoSort mouse CD4⁺CD25⁺ regulatory T cell isolation kit (Biolegend, USA), following the manufacturer's protocol. For flow cytometry analysis, the viability of splenocytes (2×10^6 cells) or CD4⁺CD25⁺ T cells was assessed using eBioscience Fixable Viability Dye eFluor 506. Following this, the cells were incubated with 1 μ g anti-CD16/32 antibody (Elabscience, USA) for 15 min to block nonspecific binding to Fc receptors. Subsequently, the cells were stained with the following surface markers for 1 h using 1 μ g primary antibodies: anti-CD3-PerCP-Cyanine5.5, anti-CD4-ER780, and anti-CD25-APC antibodies, all of which were obtained from eBiosciences. For intracellular staining, the splenocytes were first fixed and permeabilized using Foxp3 Fixation/Permeabilization Concentrate and Diluent (eBiosciences, USA) and then stained with anti-Foxp3-PE antibody (Elabscience, USA) for 2 h. The results were analyzed using a Beckman Coulter CytoFLEX-LX flow cytometer with NovoExpress software (version 1.2.5).

2.17 | Fluorescence In Situ Hybridization (FISH)

To investigate the localization of emu-let-7-5p in PBLC and splenic lymphocyte sections, *E. multilocularis*-infected BALB/c mice and age-matched controls were utilized. PBLC and splenic lymphocytes were isolated as described in Section 2.4. FISH was performed as follows: Briefly, after de-waxing, the slices were boiled in the repair solution for 15 min and naturally cooled. Proteinase K working solution (20 μ g/mL, Servicebio, China) was used to digest at 37°C for 20 min. After three washes with PBS, the sections were pre-hybridized with hybridization solution for 1 h at 37°C. Then, the emu-let-7-5p probe was incubated with the section in hybridization solution (500 nM) in a humidity chamber overnight at 40°C. After removing the hybridization solution, the sections were washed sequentially in $2 \times$ SSC, $1 \times$ SSC, and $0.5 \times$ SSC, each for 5 min at 37°C. Afterward, nuclei were stained with DAPI for 10 min. The slides were observed using a fluorescence microscopy (Nikon, Japan). The probe used in the FISH test is presented in Table S3.

2.18 | Statistical Analysis

All results were presented as mean \pm standard deviation (SD). The Student's *t*-test was used to compare differences between two groups. Figures were drawn using Graph Pad Prism 10 software. $p < 0.05$ was considered statistically significant.

3 | Results

3.1 | *E. multilocularis* Infection Induces the Upregulation of Treg-Related Nuclear Transcriptional Factors and Cytokines in Mouse PBLC and Spleen

To explore the host immune response to *E. multilocularis* infection, with a particular focus on the dynamic changes in Th1/Th2/Th17/Treg-associated cytokines, we infected mice with *E. multilocularis* protoscolices and measured the expression levels of IFN- γ , IL-4, IL-10, IL-17, TGF- β , and the Treg-specific transcription factor Foxp3 in the PBLC of the mice using RT-qPCR at 30, 60, 90, and 180 dpi. At 30 dpi, the level of the Th1 cytokine IFN- γ in the *E. multilocularis*-infected group was significantly higher than that in the control group (Figure 1A), while the level of the Th2 cytokine IL-4 was significantly increased at 60 dpi and subsequently returned to baseline levels by 90 and 180 dpi (Figure 1B). Additionally, IL-17 mRNA was also markedly elevated at 60 dpi (Figure 1C). The levels of the Treg-specific transcription factor Foxp3, along with the hallmark cytokine TGF- β , were significantly upregulated at 30 dpi (Figure 1D,E). Furthermore, the expressions of Foxp3, IL-10, and TGF- β were also significantly upregulated at 60, 90, and 180 dpi (Figure 1D-F). In contrast, the levels of IL-4 and IL-17 did not show statistically significant differences between the control and infected groups at 30, 90, and 180 dpi (Figure 1B,C). However, at 60 dpi, the difference in IL-4 between the infection and the control group was significant (Figure 1B). These results indicate that *E. multilocularis* promotes peripheral blood T lymphocytes to differentiate into Treg cells.

We conducted a detailed analysis of the percentage of CD4⁺CD25⁺ cells within CD4⁺ T cells in the spleen of the *E. multilocularis*-infected mice by flow cytometry. Our findings showed a notable increase in the proportion of splenic CD4⁺CD25⁺Foxp3⁺ Treg cells over time in the *E. multilocularis*-infected mice compared to control mice (Figure 1G,H). These results suggest that *E. multilocularis* successfully promotes the differentiation of host Foxp3⁺ Treg cells.

3.2 | Emu-let-7-5p is Upregulated in PBLC and Splenic Lymphocyte During *E. multilocularis* Infection

Previous studies have suggested that emu-let-7-5p is associated with Treg cell differentiation [27]. Therefore, we assessed the levels of emu-let-7-5p in the PBLC and splenic lymphocytes of both control and *E. multilocularis*-infected mice. Firstly, we investigated whether emu-let-7-5p was present in the PBLC and splenic lymphocytes during *E. multilocularis* infection. FISH results showed that red fluorescence was observed in the PBLC and splenic lymphocytes from *E. multilocularis*-infected mice at 60 dpi, but not in those cells from control mice, indicating that emu-let-7-5p only existed in PBLC and splenic lymphocytes from *E. multilocularis*-infected mice (Figure 2A).

The results from RT-qPCR further demonstrated a significant upregulation of emu-let-7-5p in the PBLC and splenic

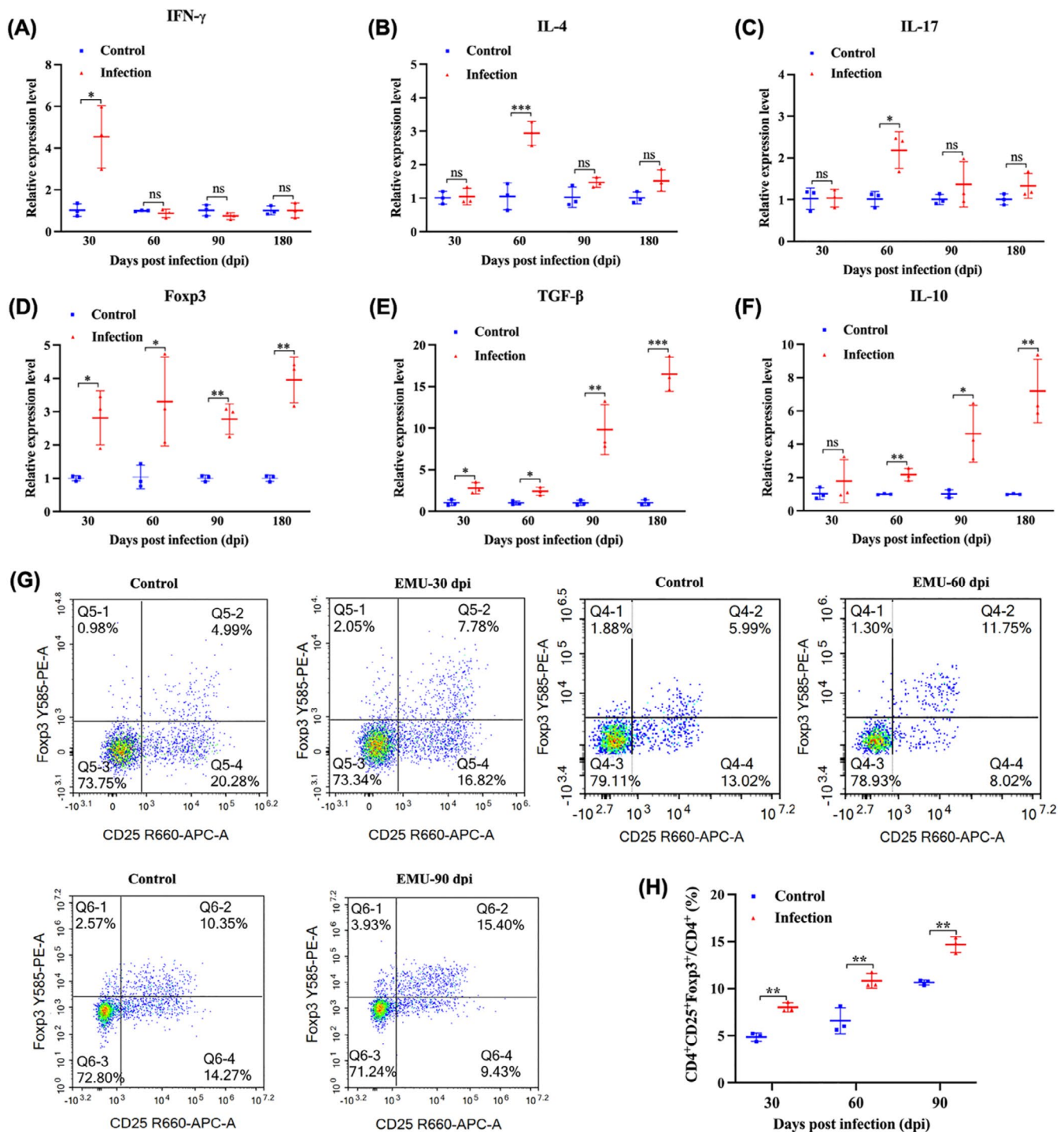


FIGURE 1 | *E. multilocularis* promotes up-regulation of Treg-related molecules in mice. (A) The expression of Th1 cytokine IFN- γ in PBLC by RT-qPCR. (B) The expression of Th2 cytokine IL-4 in PBLC by RT-qPCR. (C) The expression of Th17 cytokine IL-17 in PBLC by RT-qPCR. (D) The expression of Treg marker Foxp3 in PBLC by RT-qPCR. (E) The expression of TGF- β in PBLC by RT-qPCR. (F) The expression of IL-10 in PBLC by RT-qPCR. (G) The kinetics of splenic CD4⁺CD25⁺Foxp3⁺ Treg frequencies (as percentage of total peritoneal CD4⁺ T cells) was monitored by flow cytometry. (H) The proportion of splenic CD4⁺CD25⁺Foxp3⁺ T cells in the CD4⁺ T cell population. ^{ns} $p > 0.05$, ^{*} $p < 0.05$, ^{**} $p < 0.01$, ^{***} $p < 0.001$ vs. control.

lymphocytes of *E. multilocularis*-infected mice at 30, 60, 90, and 180 dpi (Figure 2B,C). Notably, the expression patterns of Treg-related factors were consistent with the levels of emu-let-7-5p, indicating a potential relationship between Treg cell differentiation and emu-let-7-5p level in the context of *E. multilocularis* infection.

3.3 | Knockdown of emu-let-7-5p in *E. multilocularis* Exosomes Inhibits Mouse Peripheral Blood and Splenic Treg Cell Differentiation

We investigated the roles of emu-let-7-5p in the differentiation of host Treg cells in vitro by using siRNA to knock down

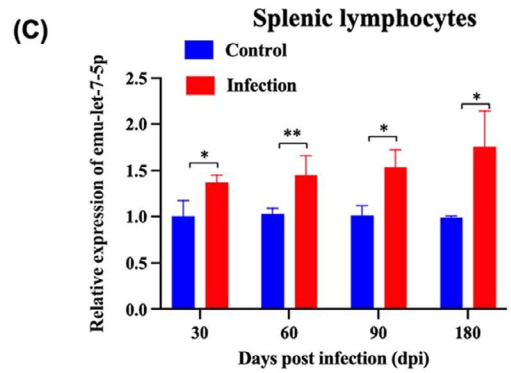
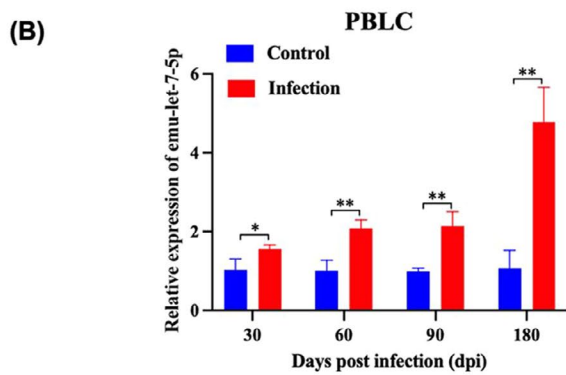
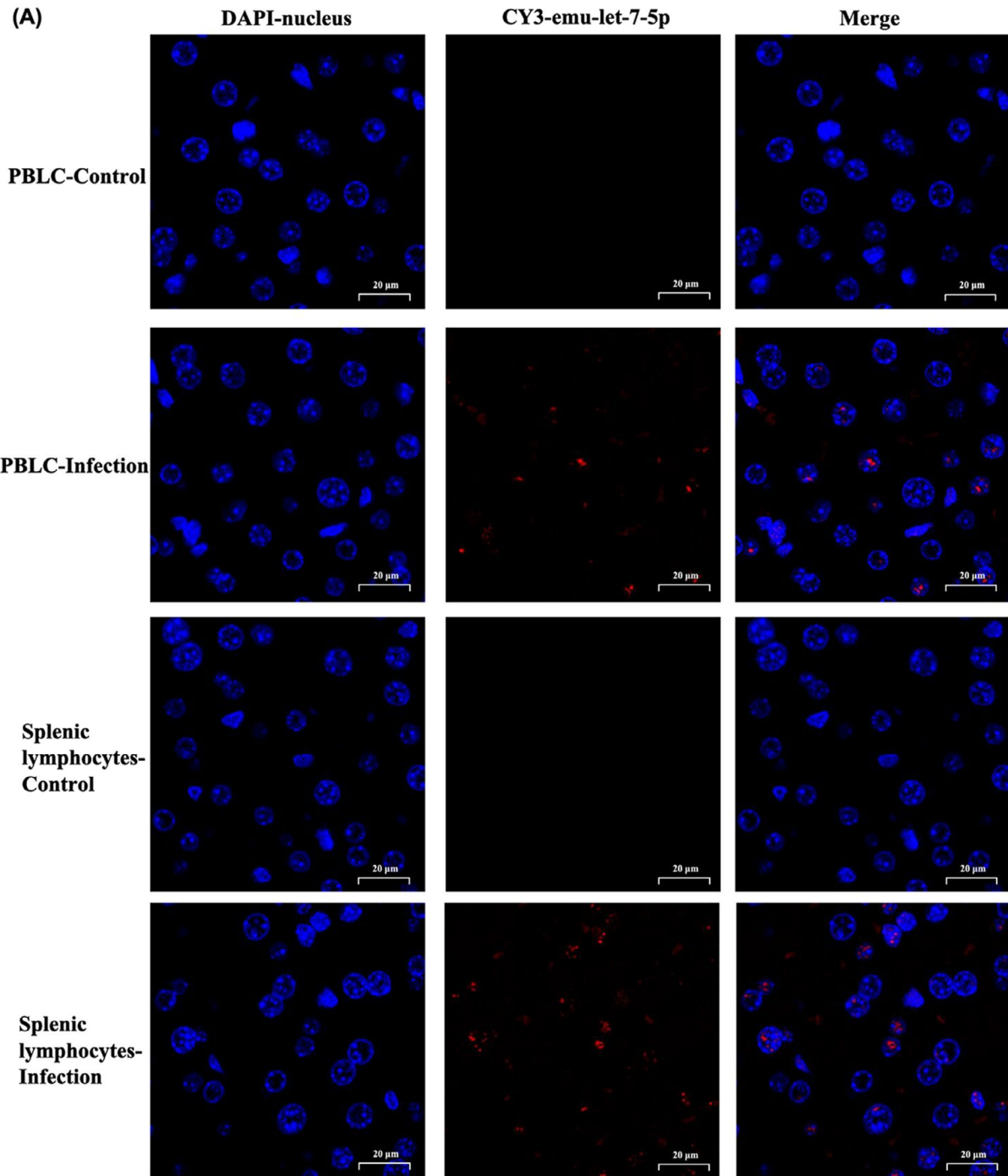


FIGURE 2 | Legend on next page.

FIGURE 2 | Analysis of emu-let-7-5p in lymphocytes of mice infected with *E. multilocularis*. (A) FISH analysis of emu-let-7-5p in PBLC and splenic lymphocytes. (B) The expression of emu-let-7-5p in the PBLC by RT-qPCR. (C) The expression of emu-let-7-5p in the splenic lymphocytes by RT-qPCR. * $p < 0.05$; ** $p < 0.01$ vs. control.

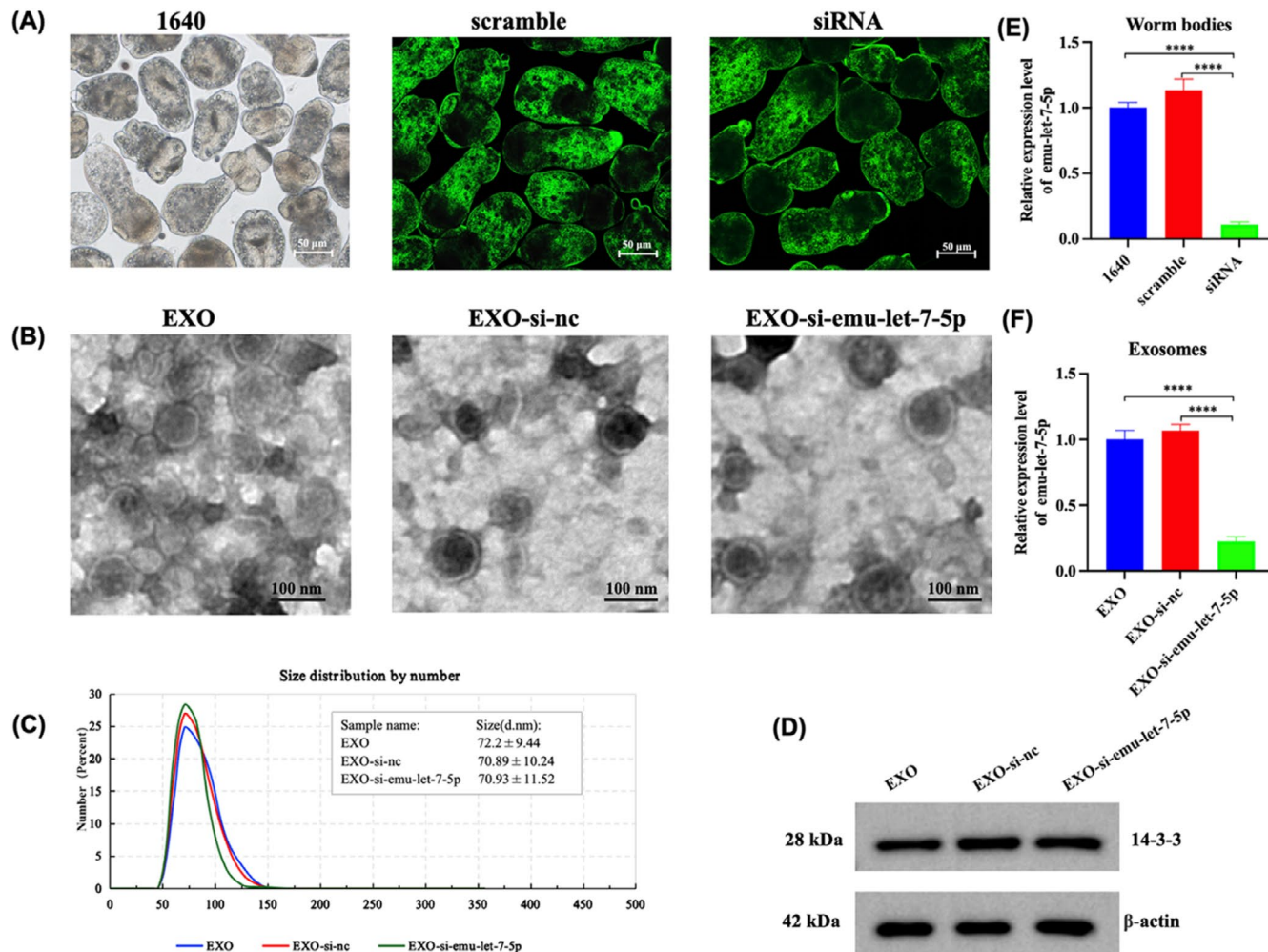


FIGURE 3 | Knockdown of emu-let-7-5p in protoscolices and exosomes from *E. multilocularis*. (A) Emu-let-7-5p specific siRNA oligonucleotide or scrambled siRNA labeled with a green dye were observed within protoscolices. (B) Morphology and structure analysis of exosomes from RPMI-1640 medium (EXO), scrambled siRNA (EXO-si-nc), and emu-let-7-5p-siRNA treated worms (EXO-si-emu-let-7-5p) by TEM. (C) The size distribution of exosomes using NTA. (D) The expression of the exosomal protein 14-3-3 by western blotting. (E) The relative expression levels of emu-let-7-5p in RPMI-1640 (1640), emu-let-7-5p-siRNA (siRNA), or scrambled siRNA (Scramble)-treated worms by RT-qPCR. (F) The interference efficiency of emu-let-7-5p in exosomes from these different treated worms by RT-qPCR. **** $p < 0.0001$.

emu-let-7-5p in protoscolices. Bright green fluorescence was observed under fluorescence microscopy in protoscolices treated with both the emu-let-7-5p specific siRNA and the scrambled siRNA, in contrast to those treated with RPMI-1640 medium (Figure 3A), indicating that the siRNA was delivered successfully into the worm bodies via electroporation. Furthermore, exosomes isolated from protoscolices treated with RPMI-1640 medium (EXO), scrambled siRNA (EXO-si-nc), and emu-let-7-5p-siRNA (EXO-si-emu-let-7-5p) were also identified, respectively (Figure 3B–D). TEM analysis showed that these vesicles had obvious lipid bilayer membranes, about 50–150 nm in diameter (Figure 3B). Furthermore, NTA showed that the size distribution of the vesicles peaked at a mean diameter of 70 nm, which meets typical morphological characteristics of exosomes

(Figure 3C). Western blot results showed that these vesicles were positive for 14-3-3 (Figures 3D and S1), which is one of the most abundant proteins in *E. multilocularis*-derived exosomes. The above results indicated that we successfully obtained the exosomes from protoscolices. The levels of emu-let-7-5p in exosomes and protoscolices were analyzed by RT-qPCR, which revealed a 90% reduction in worm bodies (Figure 3E) and a 70% reduction in exosomes (Figure 3F) derived from the protoscolices treated with emu-let-7-5p siRNA, respectively. These results suggest that emu-let-7-5p in exosomes was efficiently silenced by siRNA.

To determine the effects of exosomes on the expression of Treg cell hallmark molecules of PBLC, the exosomes, containing

endotoxin less than 0.01 EU/mL, were incubated with mouse PBLC. Confocal laser scanning microscopy observed that the DiD-labeled exosomes were transferred to mouse PBLC, mainly around the perinuclear region (Figure 4A). RT-qPCR results showed that exosomes significantly increased the expression of Treg cell hallmark molecules, such as TGF- β , IL-10, and Foxp3, in mouse PBLC (Figure 4B). Remarkably, knockdown of emu-let-7-5p in exosomes reversed the induction of Treg cell markers compared to the EXO-si-nc group (Figure 4B), which highlights that emu-let-7 is closely related to exosome-induced Treg differentiation.

We also evaluated the differentiation of splenic CD4⁺CD25⁺Foxp3⁺ Treg cells in mouse CD4⁺CD25⁺ T cells treated with PBS, TGF- β (5 ng/mL) + IL-2 (20 ng/mL), EXO (50 μ g/ μ L), EXO-si-nc (50 μ g/ μ L) or EXO-si-emu-let-7-5p (50 μ g/ μ L). Flow cytometry data revealed a remarkable increase in the proportion of CD4⁺CD25⁺Foxp3⁺ Treg cells within CD4⁺ T cells in the TGF- β + IL-2 and EXO-treated spleen cells (Figure 4C,D). Conversely, the proportion of CD4⁺CD25⁺Foxp3⁺ Treg cells within CD4⁺ T cells significantly decreased in the EXO-si-emu-let-7-5p group compared to the EXO-si-nc group (Figure 4C,D). Taken together, these data suggest that emu-let-7-5p derived from *E. multilocularis* exosomes plays a crucial role in regulating the differentiation of host Treg cells.

3.4 | The Role of the Target Gene NF κ B2 in Differentiation of Treg Cells by Emu-let-7-5p

Using TargetScan, MiRanda, and PicTar databases, we predicted 2818 potential targets of emu-let-7-5p (Table S4). Four candidates—MAP4K3, HOXB3, NF κ B2, and MAP3K7—were prioritized for experimental validation based on their documented roles in T cell differentiation pathways [37, 38] and predicted binding sites to emu-let-7-5p. To assess whether emu-let-7-5p can inhibit the expression of these mRNAs, we transfected emu-let-7-5p mimics and mimics nc into mouse PBLC and measured the expression levels of these targets via RT-qPCR. We confirmed successful transfection of emu-let-7-5p, which was approximately 160 times higher than in the control group (Figure 5A). Notably, the levels of NF κ B2 and MAP3K7 mRNA were significantly reduced in cells overexpressing emu-let-7-5p (Figure 5B). In contrast, the expressions of MAP4K3 and HOXB3 did not differ significantly between the mimics nc and emu-let-7-5p treated groups (Figure 5B). Given the more pronounced downregulation of NF κ B2 ($p=0.0005$) compared to MAP3K7 ($p=0.0183$), we chose NF κ B2 as the primary target gene for emu-let-7-5p.

Our analysis revealed two potential binding sites for emu-let-7-5p on the 3'UTR and CDS of NF κ B2, respectively (Figure 5C). To determine whether emu-let-7-5p directly regulates NF κ B2, we conducted a dual luciferase reporter assay to investigate their interaction. The results showed a significant decrease in luciferase activity in cells co-transfected with emu-let-7-5p mimics and the wild-type NF κ B2 CDS construct (CDS-WT), or with emu-let-7-5p mimics and the wild-type NF κ B2 3'UTR construct (CDS-3'UTR-WT) compared to their respective controls (Figure 5D, $p=0.004$ and $p=0.002$, respectively). The emu-let-7-5p mimics did not have a significant effect on luciferase activity in cells

co-transfected with the mutant-type NF κ B2 CDS construct (CDS-MUT) or the mutant NF κ B2 3'UTR construct (CDS-3'UTR-MUT) (Figure 5D). These findings suggest that emu-let-7-5p directly targets NF κ B2, with a more pronounced inhibitory effect observed when emu-let-7-5p binds to the 3'UTR and CDS regions of NF κ B2.

To evaluate the role of NF κ B2 in Treg cell differentiation, we measured the expression of key Treg markers in mouse PBLC transfected with pEGFP-N1, pEGFP-N1-NF κ B2, specific NF κ B2 siRNA, or scrambled siRNA. As shown in Figures 5 and S2, NF κ B2 overexpression significantly decreased IL-10 and Foxp3 levels (Figure 5E-G). In contrast, NF κ B2 knockdown notably increased the mRNA levels of TGF- β , IL-10, and Foxp3 (Figure 5E-G). These results underscore the critical role of NF κ B2 in regulating Treg cell differentiation.

3.5 | Inhibition of Emu-let-7-5p Reduces *E. multilocularis*-Induced Treg Cell Differentiation and Suppresses Parasite Growth in an Animal Model

To investigate the role of emu-let-7-5p in Treg cell differentiation during *E. multilocularis* infections, a recombinant adeno-associated virus (rAAV8-si-emu-let-7-5p) was created with a sponge sequence complementary to emu-let-7-5p (Figure 6A). The specificity and effectiveness of the emu-let-7-5p sponge vector were confirmed in HEK293T cells (Figure 6B). Mice were then injected with rAAV8 carrying either the emu-let-7-5p sponge sequence (rAAV8-si-emu-let-7-5p) or a control (rAAV8-si-control), respectively (Figure 6C). At 15 dpi, GFP expression was observed in the rAAV8-si-control and rAAV8-si-emu-let-7-5p groups but not in the PBS group, confirming effective delivery of the sponge sequence into the mouse livers (Figures 6D and S3). At 90 dpi, RT-qPCR of mouse PBLC revealed a significant decrease in emu-let-7-5p levels in the rAAV8-si-emu-let-7-5p group (Figure 6E), which was accompanied by a significant increase in the expression of NF κ B2 (Figure 6F) and a notable reduction in the transcription levels of the Treg cell-specific transcription factor Foxp3 and its associated cytokines IL-10 and TGF- β (Figure 6G-I). A similar pattern of change was observed in mouse splenic lymphocytes, where rAAV8-si-emu-let-7-5p-mediated knockdown of emu-let-7-5p resulted in significant up-regulation of NF κ B2 and decreased expression of Foxp3, IL-10, and TGF- β (Figure 6J-N). These results suggest that the emu-let-7-5p sponge sequence effectively inhibited the differentiation of Treg cells induced by emu-let-7-5p during *E. multilocularis* infections.

ELISA analysis of mouse serum further supported these results, showing significant reductions in Foxp3, IL-10, and TGF- β levels in the rAAV8-si-emu-let-7-5p group (Figure 6O-Q). Overall, knockdown of emu-let-7-5p in mice using rAAV8-si-emu-let-7-5p enhanced the expression of NF κ B2 and effectively suppressed *E. multilocularis*-induced Treg cell differentiation.

To assess the impact of Treg cell differentiation on cyst growth in the liver, we measured the weight of cysts and the number of protoscolices. The results showed a significant decrease in both the mean number of protoscolices and cyst weight in the

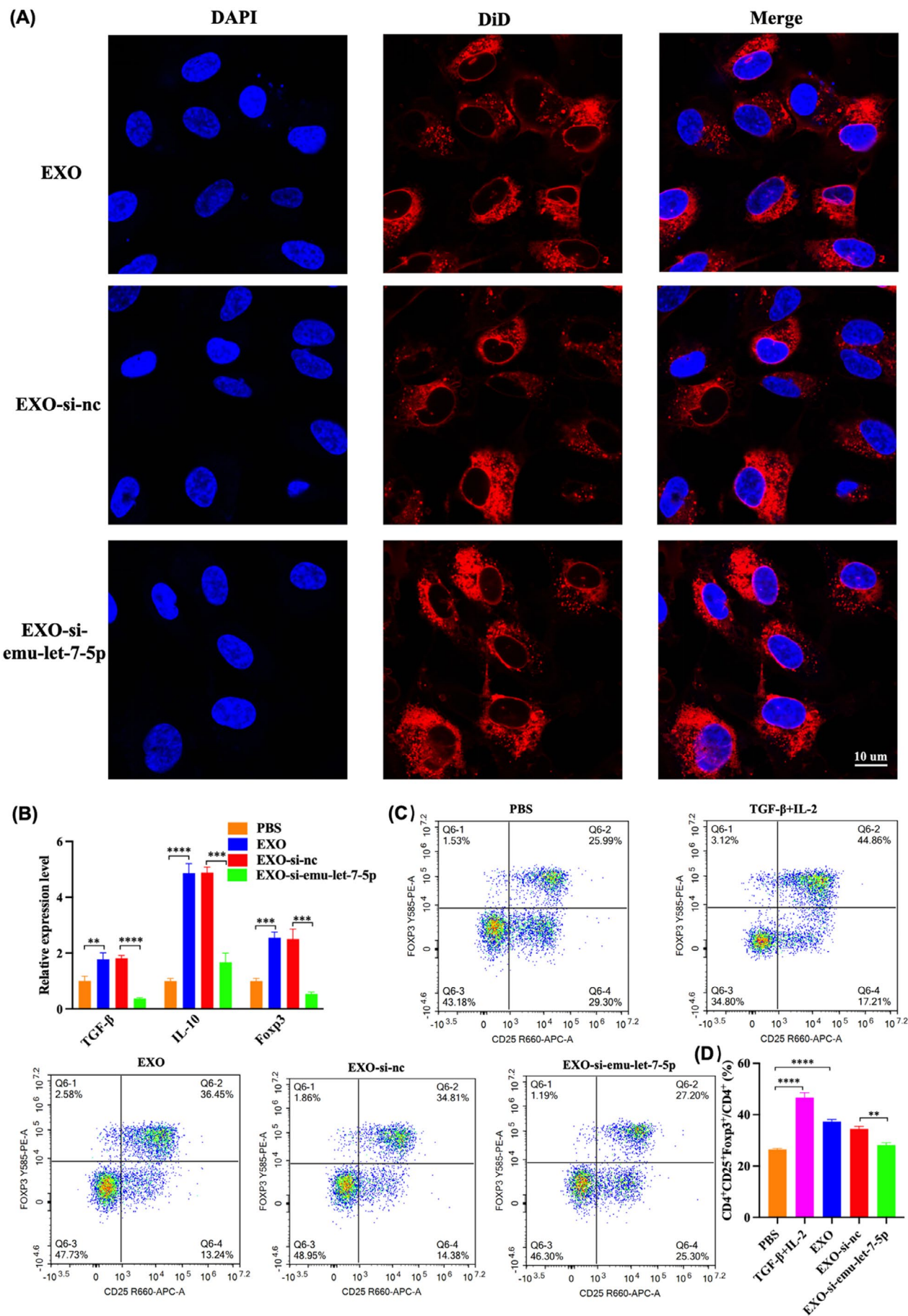


FIGURE 4 | Legend on next page.

FIGURE 4 | Knockdown of emu-let-7-5p inhibits *E. multilocularis* exosome-induced Treg differentiation. (A) Exosomes from RPMI-1640 medium (EXO)-, scrambled siRNA (EXO-si-nc)-, and emu-let-7-5p-siRNA (EXO-si-emu-let-7-5p)-treated worms were uptake by mouse PBLC. (B) The relative expression levels of TGF- β , IL-10 and Foxp3 in the mouse PBLC treated with PBS, EXO, EXO-si-nc, and EXO-si-emu-let-7-5p. (C) Splenic CD4⁺CD25⁺Foxp3⁺ Treg frequencies in CD4⁺ T cells treated with PBS, TGF- β + IL-2, exosomes from RPMI-1640 medium (EXO), scrambled siRNA (EXO-si-nc), and emu-let-7-5p-siRNA-treated worms (EXO-si-emu-let-7-5p) for 2 days. (D) The proportion of splenic CD4⁺CD25⁺Foxp3⁺ T cells in the CD4⁺ T cell population. ** $p < 0.01$; *** $p < 0.001$; **** $p < 0.0001$.

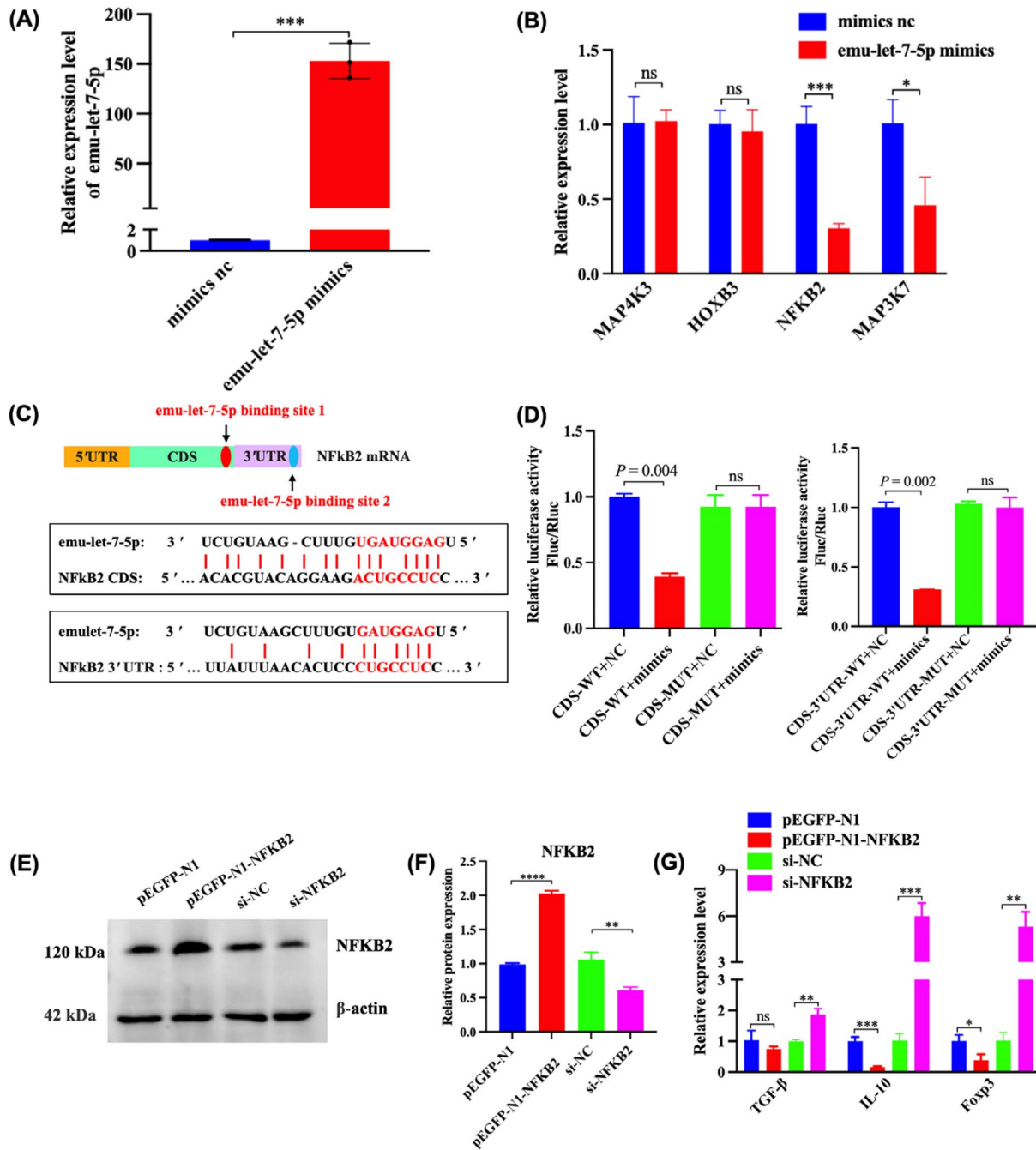


FIGURE 5 | Emu-let-7-5p regulates Treg cell differentiation through targeting NF κ B2. (A) The expression of emu-let-7-5p in mouse PBLC after transfection with emu-let-7-5p mimic for 24 h was detected using RT-qPCR. (B) The relative mRNA expression of MAP4K3, HOXB3, NF κ B2, and MAP3K7 in PBLC transfected with emu-let-7-5p mimics or mimics nc for 24 h. (C) The potential binding sites of emu-let-7-5p in the CDS and 3'UTR of NF κ B2 were predicted using the intersection of TargetScan, MiRanda, and PicTar databases. (D) Luciferase activities were measured in HEK293T cells co-transfected with the wide-type (WT) or mutated (MUT) constructs and emu-let-7-5p mimics and control, respectively. (E) Knockdown and overexpression of NF κ B2 in PBLC by western blotting. (F) Knockdown and overexpression of NF κ B2 in PBLC by RT-aPCR. (G) The relative expression levels of TGF- β , IL-10 and Foxp3 in PBLC were determined by RT-qPCR. ns $p > 0.05$, * $p < 0.05$; ** $p < 0.01$; *** $p < 0.001$; **** $p < 0.0001$.

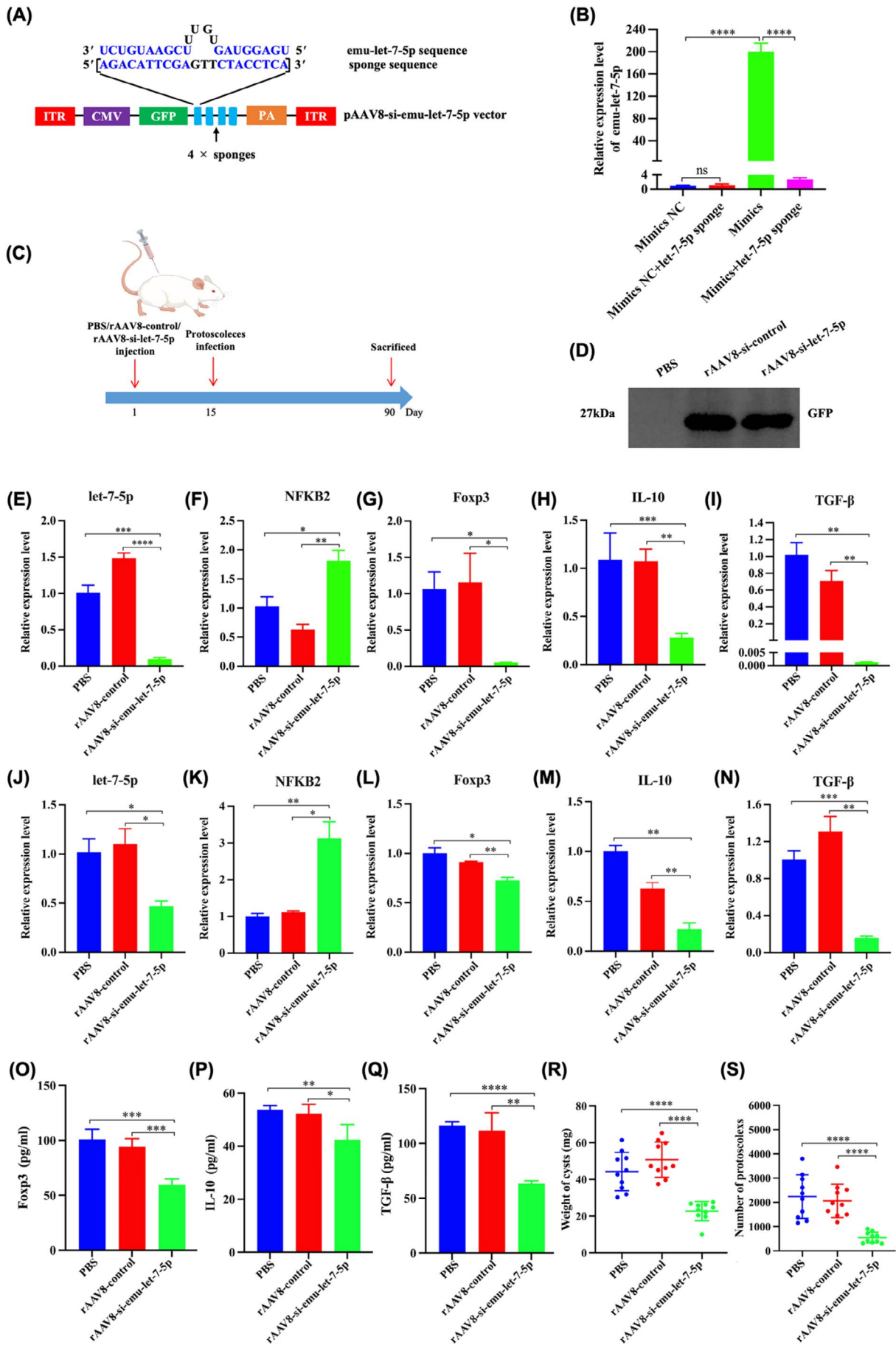


FIGURE 6 | Legend on next page.

FIGURE 6 | Knockdown of emu-let-7-5p inhibits Treg cells differentiation induced by *E. multilocularis*. (A) Construction of recombinant plasmid pAAV8-si-emu-let-7-5p. (B) Validation of the inhibitory effect of emu-let-7-5p sponge in vitro. (C) The study design of the animal experiment. (D) Expression of GFP protein in the liver of mice detected by Western blot at 15 dpi ($n=1$ per group). Expression of emu-let-7-5p (E), NF κ B2 (F), Foxp3 (G), IL-10 (H), and TGF- β (I) in mouse PBLC detected by RT-qPCR at 90 dpi ($n=10$ per group). Expression of emu-let-7-5p (J), NF κ B2 (K), Foxp3 (L), IL-10 (M), and TGF- β (N) in mouse splenic lymphocytes detected by RT-qPCR at 90 dpi ($n=10$ per group). Expression of Foxp3 (O), IL-10 (P), and TGF- β (Q) in mouse serum detected by ELISA at 90 dpi ($n=10$ per group). The total weight of cysts (R) and the number of protoscolices (S) in mouse liver at 90 dpi ($n=10$ per group). * $p < 0.05$; ** $p < 0.01$; *** $p < 0.001$; **** $p < 0.0001$.

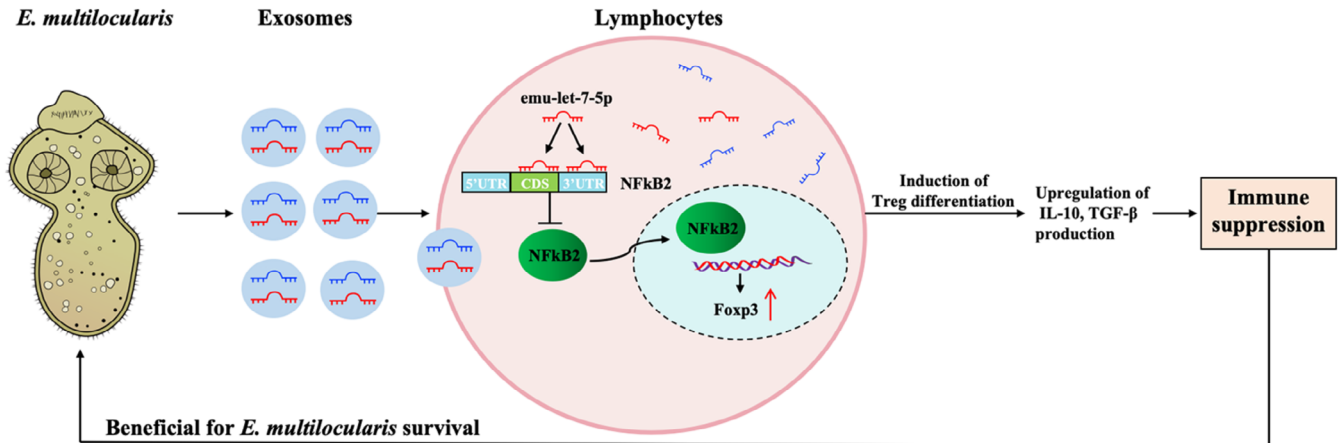


FIGURE 7 | A schematic model shows that emu-let-7-5p from *E. multilocularis* induces the host Treg differentiation. After *E. multilocularis* infection, the miRNA emu-let-7-5p induces the increase of the number of Foxp3⁺ Treg and production of the Treg-specific transcription factor Foxp3, along with hallmark cytokines IL-10 and TGF- β , by targeting the 3'UTR and CDS regions of NF κ B2.

rAAV8-si-emu-let-7-5p group (Figure 6R,S). Mice treated with rAAV8-si-emu-let-7-5p had a 73.48% reduction in worm burden (Figure 6S), which indicates that emu-let-7-5p knockdown effectively reduces *E. multilocularis*-induced Treg cell differentiation, leading to the inhibition of parasite growth.

4 | Discussion

AE is a chronic disease characterized by the malignant, tumor-like growth of *E. multilocularis* within an intermediate host organ, which can persist unnoticed for years or even decades [39]. A key strategy for *E. multilocularis* to successfully colonize its host is its ability to induce immune tolerance or suppression. Research has shown that this immune suppression is linked to the parasite's surface structures and metabolites released from *E. multilocularis* [11, 40]. Regulatory T cells are known to play a major role in helminth-induced immune suppression [16]. However, the molecular mechanisms underlying Treg cell induction by *E. multilocularis*, particularly the involvement of parasite-derived miRNAs, remain poorly understood. Therefore, elucidating how *E. multilocularis* induces Treg cell differentiation and developing inhibitors to target these molecules could significantly enhance our understanding of immune suppression in AE and improve strategies for controlling and preventing *Echinococcosis multilocularis*, thereby protecting public health and supporting economic development.

In helminth infections, Th1, Th2, Th17, and Treg cells play a crucial role in determining parasite clearance and protection by secreting specific cytokines [41]. Pang et al. observed that

mice secrete different cytokines at various stages of secondary AE infection [42]. During the early stage of infection, the immune reaction was characterized by a mixed Th1/Th2 response, with the presence of both IFN- γ and IL-4. In contrast, the late infection stage showed strong expression of Foxp3, IL-10, and TGF- β [15, 43]. Our study supported these findings, showing significantly elevated IFN- γ levels at 30 dpi, and increasing IL-17 levels at 60 dpi. Additionally, we found a significant increase in the expression of the Th2 cytokine IL-4 at 60 dpi, which then decreased at 90 and 180 dpi, contrary to previous findings and our initial assumption [3]. This inconsistency may be attributed to a time lag effect in protein modification, gene transcription, and translation [44].

Additionally, we found that IL-10, TGF- β , and Foxp3 levels in PBMCs and splenocytes increased progressively with infection duration. The decreased IFN- γ and increased levels of Foxp3, IL-10, and TGF- β in late infection stages align with observations in human AE and secondary infection models [43, 45]. Given that elevated IL-10, TGF- β , and Foxp3 are indicative of enhanced Treg differentiation [46, 47], we hypothesize that *E. multilocularis* may drive Treg cell differentiation to evade the host immune response. Helminths and their ESP potently stimulate CD4⁺CD25⁺Foxp3⁺ generation, promoting the secretion of the anti-inflammatory cytokines IL-10 and TGF- β [13, 48]. Exosomes, as an important part of ESP, have been reported to be internalized by host immune cells and play an important role in the differentiation of Treg [48]. Emu-let-7-5p is one of the top five most expressed miRNAs in *E. multilocularis* and exosomes [49]. Therefore, we hypothesized that emu-let-7-5p is involved in Treg differentiation in AE.

To determine whether emu-let-7-5p is involved in Treg cell differentiation induced by *E. multilocularis* and its exosomes, we used RNAi, an effective method for specifically silencing genes in parasites [50, 51], to knock down emu-let-7-5p in *E. multilocularis* protoscolices in this study. We successfully silenced the emu-let-7-5p gene in *E. multilocularis* protoscolices using RNAi through electroporation, achieving an approximately 90% interference efficiency—significantly higher than previously reported [52]. A previous research study has shown that electroporation can achieve 100–1 000 times greater silencing of dsRNA compared to direct soaking [53]. The difference in interference efficiency is likely due to the superior transfection efficacy of electroporation over soaking. Additionally, our dynamic observations showed that protoscolices could survive for over a month in culture, and RNAi did not significantly impact the parasite's growth, as evidenced by normal viability and scolex evagination throughout the experiment, consistent with findings by Yan et al. [53]. Thus, siRNA and electroporation do not affect parasite vitality. In addition, in this study, we found that exosomes from *E. multilocularis* significantly promoted CD4⁺ T cells to differentiate into CD4⁺CD25⁺Foxp3⁺ Treg, while the knockdown of emu-let-7-5p in exosomes significantly reversed the differentiation of Treg induced by exosomes. These results suggest that emu-let-7-5p was involved in the Treg cell differentiation induced by exosomes from *E. multilocularis*, which may be one of the strategies that metacestode use to modulate the host immune response.

miRNAs typically target the 3'UTR region of mRNAs to silence gene expression post-transcriptionally. Some studies also suggest that miRNAs can target the CDS or 5'UTR regions of protein-coding genes [54]. Interestingly, our study found that emu-let-7-5p targets both the 3'UTR and CDS regions of the NFκB2 gene, resulting in a more significant inhibition of translation compared to targeting just the CDS region. This enhanced effect may be due to the combined targeting of both regions by miRNA [55].

As a key component of the alternative NF-κB pathway, NFκB2 has been demonstrated to play a unique function in Treg development and homeostasis [56]. Grinberg-Bleyer et al. found that deletion of NFκB2 in T cells led to a significant increase in the percentage of Treg cells and the expression of the Treg activation marker Foxp3 in the spleen and surrounding lymph nodes [56]. In this study, overexpression of NFκB2 promoted Treg differentiation, while knockdown of NFκB2 inhibited Treg differentiation. This further confirms that NFκB2 plays an important role in driving Treg cell differentiation.

Our findings reveal a critical functional divergence between parasite-encoded and host miRNAs: while mammalian let-7c robustly suppresses MAP4K3 expression through canonical 3'UTR targeting in oncogenic contexts [57], our experimental data revealed that emu-let-7-5p (a phylogenetically conserved homolog encoded by *E. multilocularis*) failed to suppress MAP4K3 expression in PBLC ($p > 0.05$). This functional divergence highlights evolutionary constraints in cross-species miRNA-target interactions, potentially arising from: (i) Beyond the seed sequence (positions 2–8), nucleotides 13–16 of miRNAs enhance binding specificity and affinity to target mRNAs [58]. Sequence alignment analysis revealed that emu-let-7-5p harbors two nucleotide

substitutions (U14C and U16A, Figure S4) within this auxiliary pairing region compared to human let-7c. These alterations likely impair miRNA: mRNA duplex stability, thereby diminishing the capacity of the parasite-derived miRNA to regulate host targets. (ii) RNA-Binding Proteins (RBPs) bind to specific regions of miRNAs or their target sites, which can physically block miRNA-mRNA interactions, thereby preventing effective gene silencing by the miRNAs [59]. Future studies employing dual-luciferase assays and functional knockdown/overexpression experiments are needed to conclusively assess the roles of MAP4K3 in this context.

Parasites can evade immune attacks by secreting molecules that increase Treg and immunosuppressive cytokines, suggesting that targeting parasite-derived molecules could alter the course of infection [38, 60]. Previous studies have shown that the parasite *Heligmosomoides polygyrus*-derived molecule (Hp-TGM) mimics the ability of TGF-β to induce FOXP3⁺ Treg differentiation from human CD4⁺ T cells. These Treg showed superior stability compared to TGF-β induced Treg in an inflammatory environment, indicating *H. polygyrus*-derived Hp-TGM could be a potential therapeutic target for IBD and other inflammatory diseases [61]. Our study indicates that *E. multilocularis*-derived emu-let-7-5p can induce Treg differentiation by regulating NFκB2 expression, supporting the parasite's survival. Therefore, targeted knockdown of emu-let-7-5p could inhibit Treg cell differentiation induced by *E. multilocularis*, potentially affecting parasite growth and development. Using a recombinant adeno-associated virus serotype 8 vector expressing emu-let-7-5p sponges, we observed that knockdown of emu-let-7-5p reduced levels of emu-let-7-5p, IL-10, TGF-β, and Foxp3, while increasing NFκB2 expression. Notably, this knockdown significantly inhibited parasite growth. Further studies are needed to elucidate the precise mechanisms by which emu-let-7-5p promotes *E. multilocularis* growth.

In conclusion, our study demonstrates that *E. multilocularis*-derived emu-let-7-5p induces Treg cell differentiation by targeting the host's NFκB2 gene (Figure 7). Efficient and sustained inhibition of emu-let-7-5p via rAAV8-mediated delivery could offer a promising therapeutic strategy for AE.

Author Contributions

Conceptualization: Liqun Wang and Xuenong Luo. Methodology: Liqun Wang, Keke Wu, Yixuan Wu, and Shanling Cao. Data curation: Liqun Wang, Tingli Liu, Tharheer Oluwashola Amuda, and Shanling Cao. Software: Li Li and Tingli Liu. Validation: Liqun Wang, Keke Wu, and Guiting Pu; Formal analysis: Keke Wu and Guiting Pu; Investigation: Liqun Wang, Tingli Liu, Guiting Pu, Tharheer Oluwashola Amuda, and Shanling Cao. Resources: Li Li, Baoquan Fu, and Hongbin Yan. Writing – original draft: Liqun Wang. Visualization: Liqun Wang and Tingli Liu. Supervision: Baoquan Fu and Xuenong Luo. Writing – review and editing: Xuenong Luo, Baoquan Fu, Tharheer Oluwashola Amuda, Hong Yin, and Hongbin Yan. Funding acquisition: Liqun Wang, Xuenong Luo, and Hongbin Yan. Project administration: Xuenong Luo. All authors read and approved the final manuscript.

Acknowledgments

We thank the scientific staff at the Instrument Center of Lanzhou Veterinary Research Institute for their technical assistance.

Conflicts of Interest

The authors declare no conflicts of interest.

Data Availability Statement

All relevant data are contained within this article and the [Supporting Information](#).

References

1. S. Mahmoudi, S. Mamishi, M. Banar, B. Pourakbari, and H. Keshavarz, "Epidemiology of Echinococcosis in Iran: A Systematic Review and Meta-Analysis," *BMC Infectious Diseases* 19 (2019): 929.
2. M. Fakhar, M. Keighobadi, H. Z. Hezarjaribi, et al., "Two Decades of Echinococcosis/Hydatidosis Research: Bibliometric Analysis Based on the Web of Science Core Collection Databases (2000–2019)," *Food and Waterborne Parasitology* 25 (2021): e00137.
3. J. Wang and B. Gottstein, "Immunoregulation in Larval *Echinococcus multilocularis* Infection," *Parasite Immunology* 38 (2016): 182–192.
4. F. Niu, S. Chong, M. Qin, S. Li, R. Wei, and Y. Zhao, "Mechanism of Fibrosis Induced by *Echinococcus* spp.," *Diseases* 7 (2019): 51.
5. K. Xu and A. Ahan, "A New Dawn in the Late Stage of Alveolar Echinococcosis "Parasite Cancer",," *Medical Hypotheses* 142 (2020): 109735.
6. P. R. Torgerson, K. Keller, M. Magnotta, and N. Ragland, "The Global Burden of Alveolar Echinococcosis," *PLoS Neglected Tropical Diseases* 4 (2010): e722.
7. P. Deplazes, L. Rinaldi, C. A. Alvarez Rojas, et al., "Global Distribution of Alveolar and Cystic Echinococcosis," *Advances in Parasitology* 95 (2017): 315–493.
8. H. Wen, L. Vuitton, T. Tuxun, et al., "Echinococcosis: Advances in the 21st Century," *Clinical Microbiology Reviews* 32 (2019): e00075-18.
9. X. Xu, X. Qian, C. Gao, et al., "Advances in the Pharmacological Treatment of Hepatic Alveolar Echinococcosis: From Laboratory to Clinic," *Frontiers in Microbiology* 13 (2022): 953846.
10. B. Gottstein, P. Soboslay, E. Ortona, J. Wang, A. Siracusano, and D. A. Vuitton, "Immunology of Alveolar and Cystic Echinococcosis (AE and CE)," *Advances in Parasitology* 96 (2017): 1–54.
11. J. K. Nono, M. B. Lutz, and K. Brehm, "Expansion of Host Regulatory T Cells by Secreted Products of the Tapeworm *Echinococcus multilocularis*," *Frontiers in Immunology* 11 (2020): 798.
12. J. Wang, D. A. Vuitton, N. Müller, et al., "Deletion of Fibrinogen-Like Protein 2 (FGL-2), a Novel CD4+ CD25+ Treg Effector Molecule, Leads to Improved Control of *Echinococcus multilocularis* Infection in Mice," *PLoS Neglected Tropical Diseases* 9 (2015): e0003755.
13. M. P. J. White, C. M. McManus, and R. M. Maizels, "Regulatory T-Cells in Helminth Infection: Induction, Function and Therapeutic Potential," *Immunology* 160 (2020): 248–260.
14. T. Tuxun, J. H. Wang, R. Y. Lin, et al., "Th17/Treg Imbalance in Patients With Liver Cystic Echinococcosis," *Parasite Immunology* 34 (2012): 520–527.
15. J. Wang, R. Cardoso, N. Marreros, et al., "Foxp3+ T Regulatory Cells as a Potential Target for Immunotherapy Against Primary Infection With *Echinococcus multilocularis* Eggs," *Infection and Immunity* 86 (2018): e00542-18.
16. J. Wang, S. Müller, R. Lin, et al., "Depletion of Foxp3+ Tregs Improves Control of Larval *Echinococcus multilocularis* Infection by Promoting Co-Stimulation and Th1/17 Immunity," *Immunity, Inflammation and Disease* 5 (2017): 435–447.
17. J. K. Nono, M. B. Lutz, and K. Brehm, "EmTIP, a T-Cell Immunomodulatory Protein Secreted by the Tapeworm *Echinococcus multilocularis* Is Important for Early Metacystode Development," *PLoS Neglected Tropical Diseases* 8 (2014): e2632.
18. Y. Wang, A. Guo, Y. Zou, et al., "Interaction Between Tissue-Dwelling Helminth and the Gut Microbiota Drives Mucosal Immunoregulation," *NPJ Biofilms and Microbiomes* 9 (2023): 43.
19. S. V. Krylova and D. Feng, "The Machinery of Exosomes: Biogenesis, Release, and Uptake," *International Journal of Molecular Sciences* 24 (2023): 1337.
20. M. Nawaz, M. I. Malik, M. Hameed, and J. Zhou, "Research Progress on the Composition and Function of Parasite-Derived Exosomes," *Acta Tropica* 196 (2019): 30–36.
21. N. Wang, P. Zhou, Y. Chen, H. Qu, K. Lu, and J. Xia, "MicroRNA-149: A Review of Its Role in Digestive System Cancers," *Pathology, Research and Practice* 216 (2020): 153266.
22. D. Wang, M. Tang, P. Zong, et al., "MiRNA-155 Regulates the Th17/Treg Ratio by Targeting SOCS1 in Severe Acute Pancreatitis," *Frontiers in Physiology* 9 (2018): 686.
23. Q. Zeng, W. Liu, R. Luo, and G. Lu, "MicroRNA-181a and microRNA-155 Are Involved in the Regulation of the Differentiation and Function of Regulatory T Cells in Allergic Rhinitis Children," *Pediatric Allergy and Immunology* 30 (2019): 434–442.
24. X. Wang, J. Cao, Y. Yu, et al., "Role of MicroRNA 146a in Regulating Regulatory T Cell Function to Ameliorate Acute Cardiac Rejection in Mice," *Transplantation Proceedings* 51 (2019): 901–912.
25. J. Dong, W. J. Huth, N. Marcel, Z. Zhang, L. L. Lin, and L. F. Lu, "miR-15/16 Clusters Restrict Effector Treg Cell Differentiation and Function," *Journal of Experimental Medicine* 220 (2023): e20230321.
26. M. Li, Y. Ding, T. Tuersong, et al., "Let-7 Family Regulates HaCaT Cell Proliferation and Apoptosis via the ΔNp63/PI3K/AKT Pathway," *Open Med (Wars)* 19 (2024): 20240925.
27. F. Wang, C. Zhou, Y. Zhu, and M. Keshavarzi, "The microRNA Let-7 and Its Exosomal Form: Epigenetic Regulators of Gynecological Cancers," *Cell Biology and Toxicology* 40 (2024): 42.
28. J. Wang, X. Zhao, and Y. Y. Wan, "Intricacies of TGF-β Signaling in Treg and Th17 Cell Biology," *Cellular & Molecular Immunology* 20 (2023): 1002–1022.
29. L. Geng, X. Tang, S. Wang, et al., "Reduced Let-7f in Bone Marrow-Derived Mesenchymal Stem Cells Triggers Treg/Th17 Imbalance in Patients With Systemic Lupus Erythematosus," *Frontiers in Immunology* 11 (2020): 233.
30. M. Cucher, N. Macchiaroli, L. Kamenetzky, L. Maldonado, K. Brehm, and M. C. Rosenzvit, "High-Throughput Characterization of *Echinococcus* spp. Metacystode miRNomes," *International Journal for Parasitology* 45 (2015): 253–267.
31. Z. Cui, W. Yu, Z. Wang, et al., "Molecular Analyses of Exosome-Derived miRNAs Revealed Reduced Expression of miR-184-3p and Decreased Exosome Concentration in Patients With Alveolar Echinococcosis," *Experimental Parasitology* 260 (2024): 108734.
32. L. Wang, G. Pu, T. Liu, et al., "Parasite-Derived microRNA Let-7-5p Detection for Metacystodiasis Based on Rolling Circular Amplification-Assisted CRISPR/Cas9," *FASEB Journal* 38 (2024): e23708.
33. Y. Zheng, X. Guo, M. Su, et al., "Regulatory Effects of *Echinococcus multilocularis* Extracellular Vesicles on RAW264.7 Macrophages," *Veterinary Parasitology* 235 (2017): 29–36.
34. C. Mizukami, M. Spiliotis, B. Gottstein, K. Yagi, K. Katakura, and Y. Oku, "Gene Silencing in *Echinococcus multilocularis* Protoscolices Using RNA Interference," *Parasitology International* 59 (2010): 647–652.
35. Z. Liu, X. Guo, A. Guo, et al., "HIV Protease Inhibitor Nelfinavir Is a Potent Drug Candidate Against Echinococcosis by Targeting Ddi1-Like Protein," *eBioMedicine* 82 (2022): 104177.

36. L. Xia, F. Li, J. Qiu, et al., "Oncogenic miR-20b-5p Contributes to Malignant Behaviors of Breast Cancer Stem Cells by Bidirectionally Regulating CCND1 and E2F1," *BMC Cancer* 20 (2020): 949.
37. J. N. Chi, J. Y. Yang, C. H. Hsueh, C. Y. Tsai, H. C. Chuang, and T. H. Tan, "MAP4K3/GLK Inhibits Treg Differentiation by Direct Phosphorylating IKK β and Inducing IKK β -Mediated FoxO1 Nuclear Export and Foxp3 Downregulation," *Theranostics* 12 (2022): 5744–5760.
38. Y. Grinberg-Bleyer, R. Caron, J. J. Seeley, et al., "The Alternative NF- κ B Pathway in Regulatory T Cell Homeostasis and Suppressive Function," *Journal of Immunology* 200 (2018): 2362–2371.
39. W. Zhou, X. Li, X. Yang, and B. Ye, "The In Vitro Promoting Angiogenesis Roles of Exosomes Derived From the Protoscolices of *Echinococcus multilocularis*," *Journal of Microbiology and Biotechnology* 34 (2024): 1410–1418.
40. R. Meng, Y. Fu, Y. Zhang, Y. Mou, G. Liu, and H. Fan, "Indoleamine 2,3-Dioxygenase 1 Signaling Orchestrates Immune Tolerance in *Echinococcus multilocularis*-Infected Mice," *Frontiers in Immunology* 13 (2022): 1032280.
41. J. Wu, H. Z. Ma, S. Apaer, et al., "Impact of Albendazole on Cytokine and Chemokine Response Profiles in *Echinococcus multilocularis*-Inoculated Mice," *BioMed Research International* 2021 (2021): 6628814.
42. N. Pang, F. Zhang, X. Ma, et al., "TGF- β /Smad Signaling Pathway Regulates Th17/Treg Balance During *Echinococcus multilocularis* Infection," *International Immunopharmacology* 20 (2014): 248–257.
43. L. Jenne, J. Kilwinski, W. Scheffold, and P. Kern, "IL-5 Expressed by CD4+ Lymphocytes From *Echinococcus multilocularis*-Infected Patients," *Clinical and Experimental Immunology* 109 (1997): 90–97.
44. P. Song, N. Jiang, K. Zhang, et al., "Ecotoxicological Evaluation of Zebrafish Liver (*Danio rerio*) Induced by Dibutyl Phthalate," *Journal of Hazardous Materials* 425 (2022): 128027.
45. V. Godot, S. Harraga, I. Beurton, et al., "Resistance/Susceptibility to *Echinococcus multilocularis* Infection and Cytokine Profile in Humans. I. Comparison of Patients With Progressive and Abortive Lesions," *Clinical and Experimental Immunology* 121 (2000): 484–490.
46. P. Hsu, B. Santner-Nanan, M. Hu, et al., "IL-10 Potentiates Differentiation of Human Induced Regulatory T Cells via STAT3 and Foxo1," *Journal of Immunology* 195 (2015): 3665–3674.
47. H. C. Chuang, K. J. Chuang, P. C. Cheng, C. L. Hsieh, Y. Y. Fan, and Y. L. Lee, "Indirubin Induces Tolerogenic Dendritic Cells via Aryl Hydrocarbon Receptor Activation and Ameliorates Allergic Asthma in a Murine Model by Expanding Foxp3-Expressing Regulatory T Cells," *Phytomedicine* 135 (2024): 156013.
48. M. Siles-Lucas, R. Morchon, F. Simon, and R. Manzano-Roman, "Exosome-Transported microRNAs of Helminth Origin: New Tools for Allergic and Autoimmune Diseases Therapy?," *Parasite Immunology* 37 (2015): 208–214.
49. N. Macchiaroli, M. Preza, M. G. Pérez, et al., "Expression Profiling of *Echinococcus multilocularis* miRNAs Throughout Metacystode Development In Vitro," *PLoS Neglected Tropical Diseases* 15 (2015): e0009297.
50. J. Guerrero-Hernández, R. J. Bobes, M. García-Varela, A. Castellanos-Gonzalez, and J. P. Lacleste, "Identification and Functional Characterization of the siRNA Pathway in *Taenia Crassiceps* by Silencing Enolase A," *Acta Tropica* 225 (2022): 106197.
51. X. Zhou, Y. Hong, Z. Shang, A. M. I. Abuzeid, J. Lin, and G. Li, "The Potential Role of MicroRNA-124-3p in Growth, Development, and Reproduction of *Schistosoma Japonicum*," *Frontiers in Cellular and Infection Microbiology* 12 (2022): 862496.
52. C. Yan, Q. Y. Zhou, J. Wu, et al., "Csi-Let-7a-5p Delivered by Extracellular Vesicles From a Liver Fluke Activates M1-Like Macrophages and Exacerbates Biliary Injuries," *Proceedings of the National Academy of Sciences of the United States of America* 118 (2021): e2102206118.
53. G. Krautz-Peterson, M. Radwanska, D. Ndegwa, C. B. Shoemaker, and P. J. Skelly, "Optimizing Gene Suppression in Schistosomes Using RNA Interference," *Molecular and Biochemical Parasitology* 153 (2007): 194–202.
54. S. Kamenova, A. Aralbayeva, A. Kondybayeva, A. Akimniyazova, A. Pyrkova, and A. Ivashchenko, "Evolutionary Changes in the Interaction of miRNA With mRNA of Candidate Genes for Parkinson's Disease," *Frontiers in Genetics* 12 (2021): 647288.
55. S. Sapkota, K. A. Pillman, B. K. Dredge, et al., "On the Rules of Engagement for microRNAs Targeting Protein Coding Regions," *Nucleic Acids Research* 51 (2023): 9938–9951.
56. A. Dhar, M. Chawla, S. Chattopadhyay, et al., "Role of NF-kappaB2-p100 in Regulatory T Cell Homeostasis and Activation," *Scientific Reports* 9 (2019): 13867.
57. B. Zhao, H. Han, J. Chen, et al., "MicroRNA Let-7c Inhibits Migration and Invasion of Human Non-Small Cell Lung Cancer by Targeting ITGB3 and MAP4K3," *Cancer Letters* 342 (2014): 43–51.
58. A. Grimson, K. K. Farh, W. K. Johnston, P. Garrett-Engele, L. P. Lim, and D. P. Bartel, "MicroRNA Targeting Specificity in Mammals: Determinants Beyond Seed Pairing," *Molecular Cell* 27 (2007): 91–105.
59. P. Kundu, M. R. Fabian, N. Sonenberg, S. N. Bhattacharyya, and W. Filipowicz, "HuR Protein Attenuates miRNA-Mediated Repression by Promoting miRISC Dissociation From the Target RNA," *Nucleic Acids Research* 40 (2012): 5088–5100.
60. C. J. C. Johnston, D. J. Smyth, R. B. Kodali, et al., "A Structurally Distinct TGF- β Mimic From an Intestinal Helminth Parasite Potently Induces Regulatory T Cells," *Nature Communications* 8 (2017): 1741.
61. L. Cook, K. T. Reid, E. Häkkinen, et al., "Induction of Stable Human FOXP3+ Tregs by a Parasite-Derived TGF- β Mimic," *Immunology and Cell Biology* 99 (2021): 833–847.

Supporting Information

Additional supporting information can be found online in the Supporting Information section.